

# On the Effects of Subgrade Erosion on the Contact Pressure Distribution under Rigid Surface Structures

M. Mena<sup>1</sup>; M. A. Meguid<sup>2</sup>; and G. Assaf<sup>3</sup>

**Abstract:** The performance of rigid surface structures such as concrete pavements and slabs-on-grade supported by a deteriorated subgrade and experiencing local contact loss is investigated experimentally and numerically in this study. A laboratory setup has been designed to facilitate the simulation of subsurface erosion and measure the changes in contact pressure at selected locations under a slab-on-grade supported on granular material. The presence of erosion voids under a slab-on-grade can lead to rapid increase in the contact pressure in the immediate vicinity of the void in addition to an increase in tensile stresses at the outermost fibers of the slab. This preliminary study suggests that efforts to detect and arrest the growth of erosion voids under slabs-on-grade should be made before the voids reach the size where significant loss of support develops and the tensile strength of the slab material is exceeded.

**DOI:** 10.1061/(ASCE)GT.1943-5606.0000097

**CE Database subject headings:** Slabs; Soil erosion; Deterioration; Voids; Subgrades; Underground structures.

## Introduction

Several geotechnical engineering structures (e.g., pavements, slabs-on-grade, and footings) transfer pressure to the ground through surface contact with the supporting soil. The design of these structures usually assumes that full contact is established throughout their service life. Slabs-on-grade are usually made out of reinforced or unreinforced concrete placed on a sub-base layer over a prepared subgrade. Failure of these rigid slabs is usually attributed to two main factors. The first involves aspects related to material failure, which includes fatigue of the concrete and other construction defects. The second category is attributed to the loss in reaction support. Once a void space develops under the slab, it starts to increase due to plastic deformation of the sub-base course or subgrade, temperature curling of the slab, and subgrade erosion (Huang 1993).

Erosion of the subgrade is known to develop for many reasons, some of which are the dissolution of soluble rocks such as karst limestone (Newton 1984), dynamic loading caused by construction related activities (Tharp 1999), and the presence of nearby leaking pipes (Hauser and Howell 2001). For soil layers underlain by heavily jointed bedrock, surface water entering in the soil is

usually allowed to penetrate into the joints of the underlying bedrock causing erosion of the overburden soil. Subgrade erosion phenomenon can be very problematic when the unreinforced concrete slab experiences deformations that induce excessive tensile stresses in the outer fibers of the concrete or when the supporting soil around the void experiences excessive shear stresses. A schematic of eroded subgrade under a rigid slab-on-grade is shown in Fig. 1.

The bearing capacity of strip footings underlain by subsurface voids has been investigated by several researchers [e.g., Baus and Wang (1983)]. Results showed that, for a given void size, the bearing capacity decreased when voids were introduced immediately under the footing. This was explained by the reduction in the shear strength of the supporting system as the void became closer to the footing. Performance of concrete slabs-on-grade has also been extensively studied in the past two decades with emphasis on modes of deformation (Rajani 2002) and failure mechanisms [e.g., Mailvaganam et al. (2001)]. However, little attention has been paid to the effects of erosion voids on the distribution of contact pressure at the soil-structure interface. The objective of this study is to investigate the performance of a rigid slab-on-grade subjected to subsurface soil erosion. An experimental study is conducted to examine the changes in contact pressure during and after the erosion process. Elastoplastic finite-element analyses, validated using the experimental results, are then performed to investigate the role of void size and location on the stresses developing in the slab-on-grade and the supporting soil.

## Experimental Study

One of the challenges of the experimental program was to develop a suitable technique to simulate subsurface soil erosion underneath an existing slab-on-grade and measure the corresponding pressure at the contact surface between that slab and the soil. The physical model used in this study consisted of a rigid steel tank to contain the granular material, a mechanism to artificially simulate

<sup>1</sup>Graduate Student, Département de Génie de la Construction, École de Technologie Supérieure, 1100 Notre Dame West, Montreal, Canada PQ H3C 1K3.

<sup>2</sup>Assistant Professor, Civil Engineering and Applied Mechanics, McGill Univ., 817 Sherbrooke St. West, Montreal, Canada PQ H3A 2K6 (corresponding author). E-mail: mohamed.meguid@mcgill.ca

<sup>3</sup>Professor, Département de Génie de la Construction, École de Technologie Supérieure, 1100 Notre Dame West, Montreal, Canada PQ H3C 1K3. E-mail: gabriel.assaf@etsmtl.ca

Note. This manuscript was submitted on July 12, 2008; approved on February 2, 2009; published online on February 23, 2009. Discussion period open until March 1, 2010; separate discussions must be submitted for individual papers. This technical note is part of the *Journal of Geotechnical and Geoenvironmental Engineering*, Vol. 135, No. 10, October 1, 2009. ©ASCE, ISSN 1090-0241/2009/10-1538-1542/\$25.00.

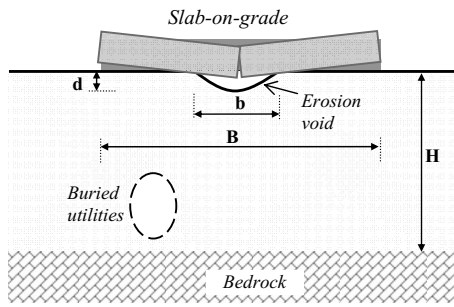


Fig. 1. Problem statement

the subsurface volume loss, and an instrumented rigid steel plate. As shown in Fig. 2, the tank was approximately 1.2 m high, 1.5 m wide, and 0.3 m thick with a 6-mm Plexiglas face. Both the front and rear sides were reinforced using three 100-mm HSS sections. The internal sides of the tank were painted and lined with plastic sheets to reduce friction between the sand and the sides of the tank.

To simulate subsurface soil erosion under the existing slab, a trap door installed at the base of the tank was used in this study. The trap door consisted of two sliding plates controlled using a threaded bolt and nut mechanism. The plates cover a symmetrical rectangular opening at the base of the tank. A 5-mm-wide opening has been used throughout this study to induce a known volume loss at the bottom of the tank. This opening size was found to provide sufficient control over the sand movement. A small container was placed directly under the tank using a hydraulic jack to control the volume of the collected sand and to maintain a constant volume loss throughout the experiments. A steel plate was used to simulate the rigid slab-on-grade. The length, width, and thickness of the steel plate were 1.4, 0.3, and 6 mm, respectively. The steel plate was reinforced using two 50-mm HSS sections welded along the length of the plate to increase its rigidity. The contact pressure was measured using two load cells (Scaim-AL 5kg) connected to a data acquisition system. The two load cells were installed flush with the bottom of the slab at a distance of 0.23 m and from the lateral boundary ( $\pm 0.5$  m from the trap door centerline). This was far enough away to allow for continuous contact between the load cell and the sand surface even after void development. Details of the load cell installation are shown in Fig. 3. Two *L-gauge* type laser sensors (Model LG5A65NIQ) were used to measure the surface settlements at two locations along the width of the tank, namely, 0.60 and 0.75 m (at the centerline) from the lateral boundary. Each transducer was fixed to a steel bracket and screwed to an alumi-

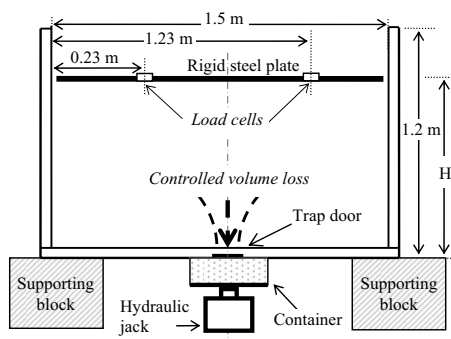


Fig. 2. Schematic of the test setup

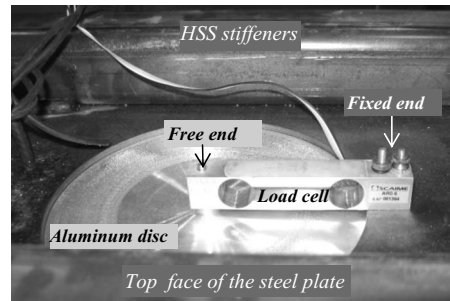
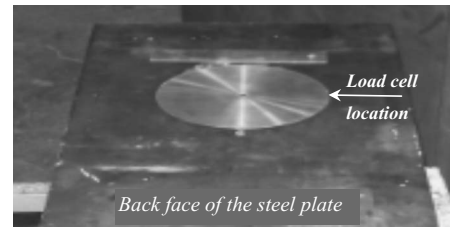


Fig. 3. Details of load cell installation

num bar that can be lowered to within a certain distance above the sand surface.

**Procedure.** A testing procedure was developed to ensure consistent initial conditions (i.e., sand density) throughout the conducted experiments. The sand was rained from a constant height into the tank in several layers (0.18 m thick) and each layer was graded to level the surface. The placement procedure was repeated until the sand surface reached the desired height,  $H$  (Fig. 1). Sieve analyses conducted on selected samples of the sand indicated a coarse-grained material with no fines. The unit weight of the sand was measured by placing small containers of known volume at different depths inside the tank. The average unit weight across the tank was found to be about  $15 \text{ kN/m}^3$ . A summary of the soil properties is given in Table 1.

Two sets of experiments were conducted. The first set was performed on the prepared sand with no steel plate at the surface. This set of experiments allowed for the surface movement profile to be measured. The test was repeated five times using sand heights of 0.18, 0.34, 0.5, 0.64, and 0.8 m to examine how the depth of initiation of the soil erosion affects the shape and size of the void that develops. The second set of experiments was conducted using the same sand heights and placement procedure. However, the steel plate was placed at the surface (weight = 436 N) inducing a pressure of approximately 1.1 kPa (as measured by the load cells). It should be emphasized that a constant volume loss has been used in all the conducted experiments.

Table 1. Soil Properties

Property	Value
Specific gravity	2.65
Coefficient of uniformity ( $C_u$ )	3.6
Coefficient of curvature ( $C_c$ )	0.82
Maximum dry unit weight ( $\gamma_{\max}$ )	$16.4 \text{ kN/m}^3$
Minimum dry unit weight ( $\gamma_{\min}$ )	$14.2 \text{ kN/m}^3$
Experimental dry unit weight ( $\gamma_d$ )	$15 \text{ kN/m}^3$
Unified soil classification system	SP
Internal friction angle ( $\phi$ )	$31^\circ$
Cohesion ( $c$ )	0.0 kPa

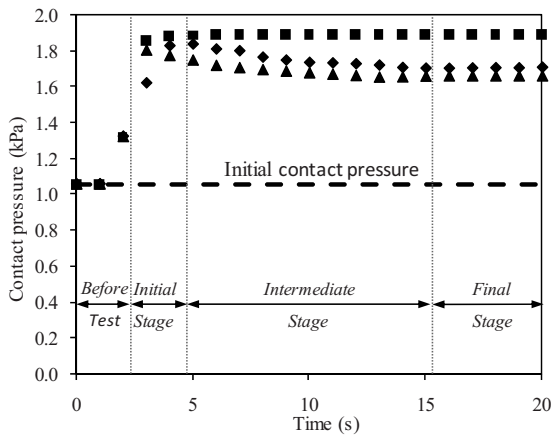


**Fig. 4.** Measured changes in contact pressure with time ( $b = 0.58$  m,  $d = 12$  mm)

**Surface Movements.** The experiments revealed that the void width,  $b$ , increases as the sand height,  $H$ , increases, reaching a maximum of  $b = 0.58$  m. Because the volume loss was held constant, the void depth,  $d$ , decreases as the void width increases, leading to a broader but shallower void at greater soil heights.

**Contact Pressure.** Fig. 4 shows the changes in contact pressure as measured in three tests conducted using a sand height of 0.8 m. The results are compared with the initial measured value (1.1 kPa) before the sand removal. It can be seen that during the process of void formation, contact pressure increased up to a peak approximately 1.8 times the initial pressure. This is followed by an intermediate stage where the contact pressure slightly changed and reached the final stage, as shown in Fig. 4. Similar results were measured at the opposite side of the void, therefore, the results for only one side are presented. It should be noted that the magnitude of the measured pressure depends on the location of the pressure cells with respect to the boundaries of the induced void. It is expected that contact pressure redistributes such that it reaches a maximum value near the edges of the void and decreases with distance until the initial contact pressure is reached. This will be further discussed in the following section.

## Numerical Analysis

Finite-element analyses have been conducted to evaluate the effects of void size on the contact pressure and the tensile stresses developing in the lower fibers of the slab. The analyses were performed using the Plaxis 8.6 2-D finite-element code. A cross section of the rigid tank hosting the sand and the steel plate was analyzed. The soil was modeled using Mohr-Coulomb failure criterion with the following parameters: friction angle =  $31^\circ$ ; dilation angle =  $0^\circ$ ; elastic modulus = 20 MPa; Poisson's ratio = 0.3; coefficient of earth pressure at rest = 0.5. The steel plate was modeled as a linear elastic material with flexural rigidity,  $EI$ , of  $10,000$  kN m<sup>2</sup>/m and normal stiffness,  $EA$ , of  $3.0 \times 10^9$  kN/m. The strength parameters of the sand were measured using direct shear tests conducted on sand samples, whereas the deformation parameters were estimated based on the available soil properties (grain size, relative density, and stress level).

The boundary conditions were selected to represent smooth rigid side boundaries and a rough rigid base boundary. Triangular solid elements with 15 nodes were used throughout the analysis.

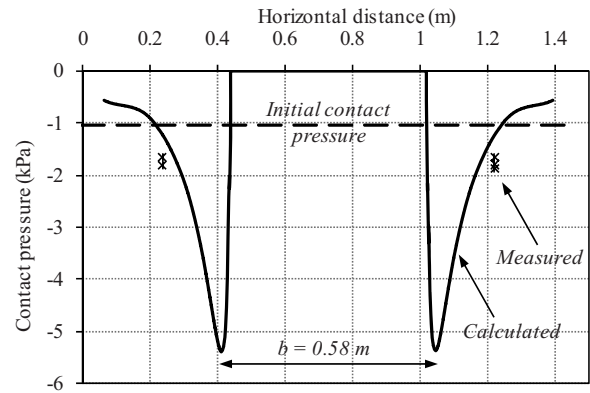


**Fig. 5.** Comparison between experimental and numerical results

The interaction between the plate and the soil is modeled using interface elements which allow for the interface condition to be simulated. A strength factor  $R_{int}$  is introduced to define the strength parameters of the interface relative to those of the sand material. A sensitivity analysis was conducted to examine the effect of varying  $R_{int}$  from 1 (rough interface) to 0 (smooth interface) and was found to have an insignificant effect on the calculated pressure. In this study, an  $R_{int}$  value of 1 has been adopted. The effect of the void location has also been investigated by examining voids forming under the centerline and the edge of the plate.

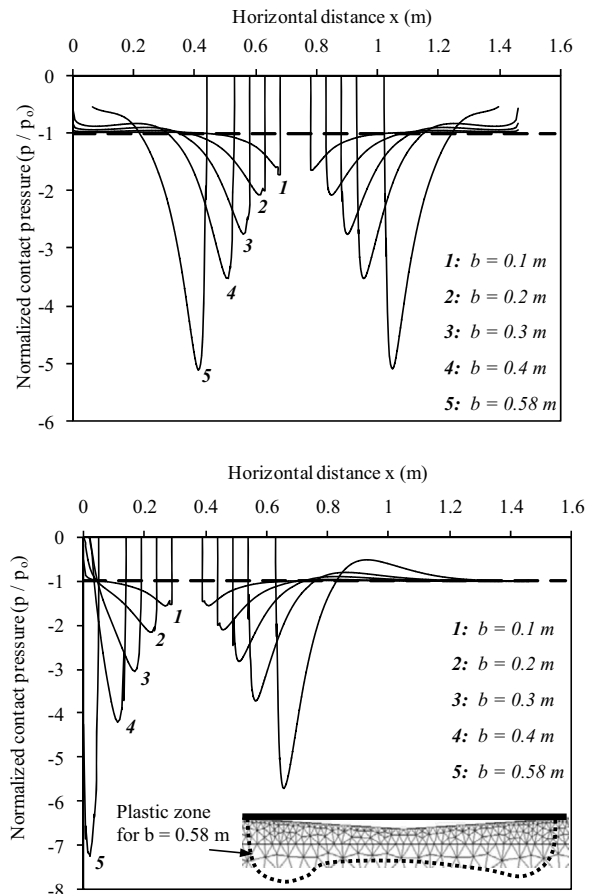


**Fig. 6.** Contact pressure distributions calculated around center and edge voids

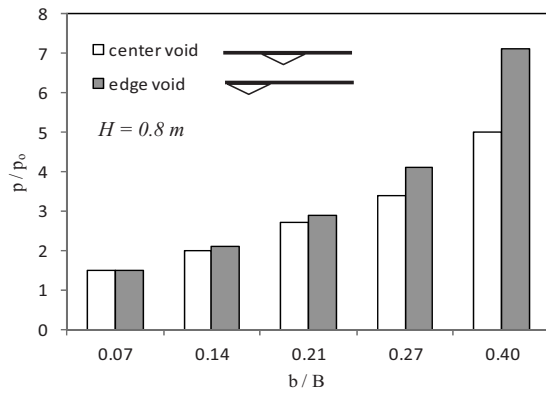


Fig. 7. Summary of contact pressure increase around voids

**Comparison with Experimental Results.** The finite-element analyses allowed for the calculation of the contact pressure at the interface between the plate and the soil after the complete formation of the void. Fig. 5 shows the redistribution of the vertical stresses with horizontal distance for a surface void of a width,  $b$ , of 0.58 m. In addition, the experimental measurements taken at 0.23 and 1.23 m are also plotted. It can be seen that, although the calculated pressures at these locations are smaller compared to the measured values, they are in general agreement given the rapid rate of pressure change around the void.

**Effect of Void Size on Contact Pressure and Stresses in the Slab.** A series of analyses was performed using the above geometry and material properties. Fig. 6 shows the contact pressure for five different void sizes ( $b=0.1, 0.2, 0.3, 0.4$ , and  $0.58$  m). The maximum contact pressure,  $p$ , is normalized with respect to the initial value ( $p_0=1.1$  kPa). In general, the pressure intensity increases very rapidly at the void boundaries and reaches a maximum value of approximately five times the initial pressure for the center voids and about seven times the initial value for the edge voids. This increase in contact pressure can reach critical values that exceed the shear strength of the soil leading to the development of a plastic zone around the void, as shown in Fig. 6. This, in turn, causes additional plastic deformation at the void edges and further loss in contact between the slab and the supporting soil. Results of the above analyses are summarized in Fig. 7 for the two cases, where the induced void is located at the centerline and at the edge of the plate. The void width,  $b$ , is normalized with respect to the width,  $B$ , of the plate. It can be seen that the contact pressure increases in a nonlinear fashion as the void size increases.

**Effect of Void Size on Stresses in the Slab.** The changes in the tensile stresses at the lower fibers of the slab (expressed by the ratio between  $\sigma_t$  after the voids develop to the initial value,  $\sigma_{t_0}$ ) are presented in Fig. 8 for different applied pressures. Tensile stresses generally increased as the void width increased. For the examined range of void sizes, the intensity of the surface loading was found to have a small effect (less than 20%) on the  $\sigma_t/\sigma_{t_0}$  ratio. Soil failure occurred for the case of a surface pressure of 140 kPa when the width of the void exceeded 0.1 m ( $b/B=0.06$ ) and, therefore, only one value is presented in Fig. 8. It has also been observed that the order of tensile stress levels varied as the void size increased. This is attributed to the plastic zone development that occurs with the increase in void size under high stress levels. The increase in tensile stresses above the initial values, assuming full contact, can lead to conditions where tensile stresses exceed the tensile strength of the slab leading to cracking

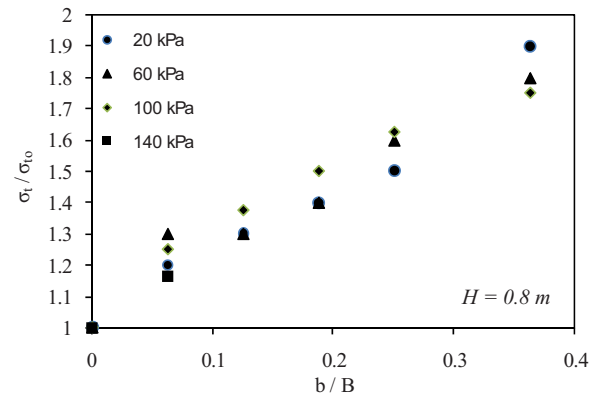


Fig. 8. Increase in tensile stresses in the lower fibers of the slab

and possibly failure. It should be emphasized that the calculated tensile stresses may vary depending on the relative stiffness between the slab and the supporting soil. Therefore, the results presented in Fig. 8 may differ from those that develop in a concrete slab with a different flexural rigidity than the steel slab used in the present analysis.

## Conclusions

Experimental and numerical investigations were conducted to examine the effects of void formation under slabs-on-grade on the contact pressure acting on the supporting soils. The development and growth of voids under the slab was found to have a significant impact on the contact pressure around the void. Tensile stresses were found to increase at the lower fibers of the slab due to loss of contact with the supporting soil. This preliminary study suggests that the efforts to detect and arrest the growth of erosion voids under slabs-on-grade should be made before the voids reach the size where significant loss of support develops and the tensile strength of the slab material is exceeded. It should be noted that the distribution of the initial contact pressure before erosion voids form may vary depending on the type and uniformity of the supporting soil. Therefore, the above results represent the cases where the initial contact pressure is uniform. Additional research is therefore needed to evaluate the effect of the nonuniformity of the initial contact pressure on the stress redistribution under slabs-on-grade.

## Acknowledgments

This research is supported by the Natural Sciences and Engineering Research Council of Canada (NSERC) (Grant No. 311971-06).

## References

- Baus, R. L., and Wang, M. C. (1983). "Bearing capacity of strip footing above void." *J. Geotech. Engrg.*, 109(1), 1-14.
- Hauser, E. C., and Howell, M. J. (2001). "Ground penetrating radar survey to evaluate roadway collapse in northern Ohio." *Proc., Symp. on Application of Geophysics to Environmental and Engineering Problems (SAGEEP)* (CD-ROM), SAGEEP, Denver, 7.

- Huang, Y. H. (1993). *Pavement analysis and design*, Prentice-Hall, Englewood Cliffs, N.J.
- Mailvaganam, N. P., Springfield, J., Repette, W., and Taylor, D. (2001). "Curling of concrete floor slabs on grade-causes and repairs." *J. Perform. Constr. Facil.*, 15(1), 11–16.
- Newton, J. G. (1984). "Review of induced sinkhole development." *Proc., 1st Multidisciplinary Conf. on Sinkholes*, B. F. Beck, ed., Balkema, Rotterdam, The Netherlands, 3–9.
- Rajani, B. (2002). "Behaviour and performance of concrete sidewalks." *Construction Technology Update No. 54*, Institute for Research in Construction, National Research Council of Canada (NRC), Ottawa, Canada.
- Tharp, T. M. (1999). "Mechanics of upward propagation of cover-collapse sinkholes." *Eng. Geol. (Amsterdam)*, 52(1–2), 23–33.